SOC governed algorithm for an EV Cascaded H-Bridge connected to a DC charger

Giulia Tresca[1], Andrea Formentini[2], Filippo Gemma [1], Federico Lusardi[3], Riccardo Leuzzi[1], Pericle Zanchetta[1,4]

[1] Electrical, Computer and Biomedical Engineering Dept., University of Pavia, Pavia, Italy

[2] Telecommunications Engineering and Naval Architecture Dep., University of Genova, Genova, Italy

[3] MTA S.p.A (Power Electronics BU), Italy

[4] Electrical and Electronic Engineering Dept.,Nottingham, University of Nottingham, Nottingham, , United Kingdom

Abstract

Cascaded H- Bridge (CHB) converters have been considered valid candidates for replacing the two-level inverter in EV powertrain applications. This paper presents a State of Charge-governed algorithm for charging Li-Ion battery modules within a Cascaded H-Bridge converter for EV powertrain, connected to a DC charger. The novelty of this algorithm lies in the balanced and concurrent charge of the battery modules installed in all submodules of the three-phases, with no extra middle stage converter needed. Simulation and experimental results are shown to prove the validity of the novel architecture and the experimental setup is described.

Keywords

«Battery modules», «Cascaded H- Bridge», «Charging algorithm», «Charging protocol», «Multilevel converter»

I. Introduction

Battery energy storage systems (BESS) play a strategic role for the Green Deal challenges that the world is approaching to face. One of the fields mostly affected by this challenge is the automotive one, where studies on new EV powertrain configurations are carried out.

Multilevel converters have been considered one of the main candidates for replacing and improving the classical 2-level inverter topology. The main benefits are better efficiency at partial loads, enhancement of the fault tolerant strategies and more flexibility in the design thanks to their modularity [1]-[3]. Moreover, the current trend to increase the DC link voltage for electrical powertrain requires urgently to define new solutions able to not stress the devices and improve the power quality without increasing losses: the modular structure of multilevel converters can guarantee both these requirements [4].

In [3], a Cascaded H-Bridge is compared with an IGBT and a SiC 2-level inverters, showing that the efficiency and the power density are comparable. In [5], a Modular Multilevel converter is proposed as valid topology for an electrical powertrain. In [6], the multilevel converter is mixed with a reconfigurable structure in order to optimally manage each battery cell.

Beside the motoring phase studies, a parallel research focus has been developed around the charging techniques for battery modules connected in multilevel configuration. Several research works in literature propose multilevel converters as the preferred topology to be installed within the charging stations because of their capability to face the grid high voltage thanks to their modularity [7]-[8]. A smaller number of research studies are focused on battery charging algorithms using multilevel converters within the electrical powertrain.

The authors of studies regarding charging processes for multilevel converters propose a direct connection between grid and converter [9]-[13]. In case of three-phases converters, each phase of the motor is connected to one phase of the grid and the single submodules are charged via customized modulations. In [9], the authors propose to use the power factor and the SOCs of the batteries to select

the best switching state. On the other hand, [10] calculates the optimal switching states for the SOC balancing. Moreover, [11] proposes two other strategies to improve the efficiency of the charging process: the first one calculates the active power, exchanged between the grid and the converter, and uses it to predict the optimal switching state to balance the SOC of the battery modules; the second one uses the AC input current to calculate the best switching states each quarter of period. Despite the latest trend foresees to perform the charging process directly from the grid, as V2G (Vehicle tom Grid), the most common charging infrastructure is characterized by a DC charger [8], which manages the full control of the power flow to the battery pack. Therefore, it is timely to define charging strategies for three-phases multilevel converters connected to a DC source. In [12], a hybrid multilevel three-phase topology is presented and a DC source is considered to perform the charging process of the battery modules connected within the converter. However, the DC source is connected in parallel to one phase at the time; therefore the charging process is divided in three different time intervals, reducing the control complexity.

This paper proposes a State of Charge (SOC) governed algorithm for a CHB connected in parallel to a DC charger, as it is shown in Fig.1a. The real novelty of this work is the simultaneous charging process for all the battery modules installed within the three phases of the converter. The algorithm implements both the control of the charger output voltage and current and the CHB submodules in order to guarantee a balanced charging process. The paper is structured as follows. Section II gives an overview about the converter structure and charging protocol adopted. Section III explains in detail the charging algorithm implemented. In section IV and V, the simulation and experimental results are shown, respectively. Section VI concludes the paper.

II. CHB structure and charging protocol

The CHB converter considered for the charging algorithm is shown in Fig.1a. Each phase has *n* submodules (SM) made of one H-bridge connected to a battery module. When the CHB is in motoring phase, the switches K1, K2, K3 and K4 are turned on and K5, K6 and K7 are turned off. Vice-versa, for the charging process, K5, K6 and K7 are turned on to connect the CHB in parallel to the charger and disconnect the motor.

Charging protocol

The key points for a valid charging protocol are a good utilization of the capacity, high energy efficiency and a short charging time. In [14], different charging protocols are discussed and analysed. The reference protocol for this algorithm is the so-called Constant Current Constant Voltage (CC - CV) charging, which is divided in two main stages:

1) In the first phase, the battery cell is charged with a constant current value I_{ch}, until its voltage reaches a specified value, defined by the datasheet.
2) In the second and last phase, the cell voltage is charged with a constant voltage equal to V_{ch} . As a consequence, the charging current exponentially decreases. Usually, V_{ch} is equal to the maximum voltage of the battery cell. The CV phase stops when the charging current drops below a predefined value, defined by the datasheet, or after a pre-determined maximum charging time.

In an equivalent way, it is possible to divide the two phases of the charging process using as key parameter the State of Charge (SOC) of the battery modules. It is common practice to lead the constant current phase until the battery module reaches a SOC value equal to SOC_{th} and then continue with the Constant Voltage phase until the current value drops below a certain value. SOC_{th} is decided in order to obtain an initial charging current in the CV phase less or equal to the one employed during the CC phase. Fig.1b shows the current and voltage behaviour during the selected charging protocol.

III. Balanced Charging Algorithm

The charging algorithm proposed in this paper is the combination of a coherent utilization of the H-bridge converter configurations and a simultaneous control of current and voltage of the DC charger.

When the battery cell needs to be charged, the H-bridge is set in the active configuration (AC), shown in Fig.2a. On the other hand, if the battery cell does not need to be charged, the H-bridge converter is set to the bypass configuration (BC), shown in Fig.2b.
The voltage and current controls are carried out to fulfil the CC and CV charging phases.

Algorithm phases

The initial SOC value is calculated by measuring the initial open-circuit voltage of the batteries and inserting it within the characteristic SOC- V_{ocp} curve, provided by the battery datasheet. Once the initial SOC is known, while the evolution of the SOC of each battery module is calculated with the Coulomb counting [15]:

$$SOC(k+1) = SOC(k) + \frac{i(k)\eta}{3600 * C_n} Ts \quad (1)$$

Where i(k) is the current flowing in the battery module at the k^{th} instant, C_n is the capacity of the battery module, T_s is the discretized time interval between k and k+1 and η is the efficiency of the charging transformation.
For the sake of simplicity, η is considered equal to 1.

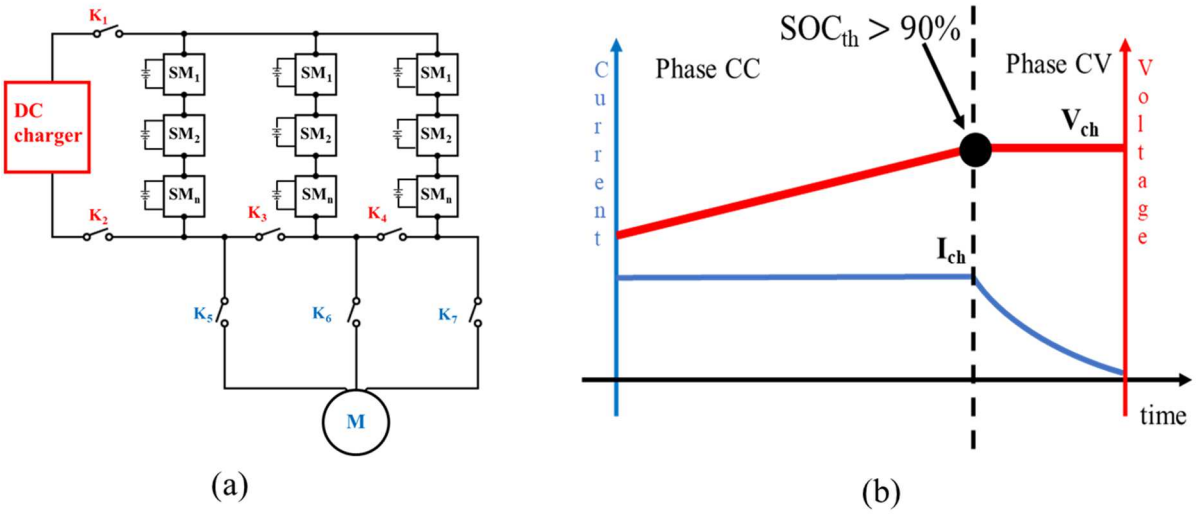

Fig. 1 – (a) CHB converter configuration for both motoring and charging phases. (b) Charging protocol CC – CV stages.

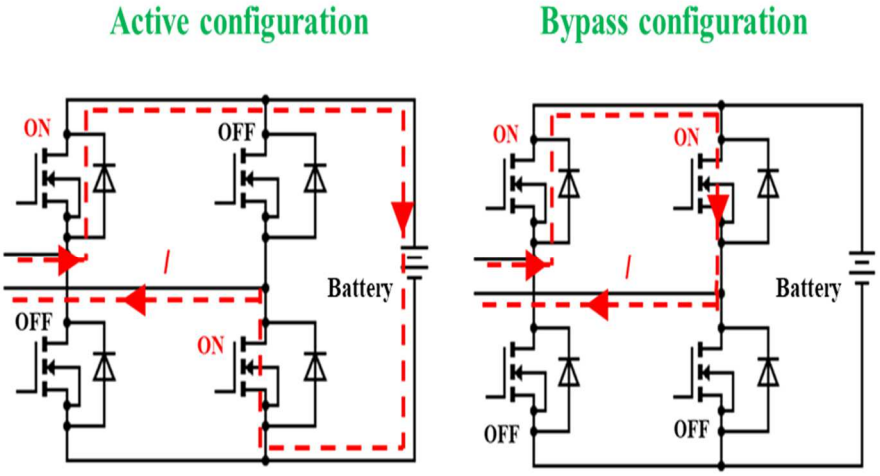

Fig. 2 – (a) shows the active configuration; (b) shows the bypass configuration. In (a), the current charges the battery module. In (b), the battery module is completely bypassed and therefore not charged.

Assuming to have *n* submodules connected in series per phase, the SOC value of the battery modules connected to the H-bridges determines the algorithm procedure.

1) All battery modules have SOC values below SOC_{th}

The H-bridges are set in active configuration, as shown in Fig. 3a, and all battery modules are charged. The output voltage of the charger is controlled in order to have a current flowing in the less charged phase equal to I_{ch}. Therefore, the other two phases will be charged with a smaller current – presenting a higher equivalent impedance.

2) m battery modules reach SOC_{th}

The *m* submodules are set in bypass configuration, as shown in Fig.3b, so that the relative battery modules are excluded from CC phase. However, an optimized current control needs an equal number of submodules per phase in active configuration. Vice versa, the current flowing in the three phases would be totally biased toward the less charged phase, provoking an unbalanced charging dynamic. Therefore, the other two phases will have a total number of submodules in active configuration equal to *n-m*. For these phases, the submodules will be set periodically in active configuration, so that the charging process can be performed in uniform way for all the battery modules.

3) All battery modules have a SOC value equal to SOC_{th}

The charger provides a fixed voltage and all submodules are set in active configuration, as shown in Fig.3c. The CV phase ends when the global current drops below a defined value.

Maximum current control

According to the phase of the charging algorithm, the implemented control is different, as it is shown in Fig.4.
When the CC phase is performed, the variable under control is the current flowing in the battery modules. However, the utilization of a unique DC voltage source makes possible the control of only one phase current. The charger voltage output needs to be optimally controlled to not create over current phenomena in any of the battery modules connected, but still allows a fast-charging process.
This result is achieved by using as control feedback variable the maximum current flowing in the three phases, obtaining two main benefits:

1) the over-current phenomena are completely avoided because the PI calculates a voltage able to guarantee the maximum current equal to the reference value. The currents flowing in the other two phases will be equal to lower values;
2) the maximum current is flowing in the less charged phase – the equivalent impedance is the lowest between the three phases. Therefore, the less charged modules will be charged faster than the other two phases, leading to a balanced charging dynamic.

The maximum current control forces only the current of the less charged phase to be constant. The other two phases perform an equivalent constant voltage charging process, with an increasing current flowing. When the CV phase is performed, the current control is replaced by the voltage control: the DC output voltage of the charger is set to the sum of the maximum voltage of the battery modules connected in one phase. Even in the case the CV would start with a minimum difference of SOC between the battery modules of the three phases, the global current would split consequently to reduce the SOCs gap between the three phases. When all phase currents drop below a certain value I_{cv} defined by the datasheet, the CV phase is terminated and the DC charger voltage is nailed to zero.

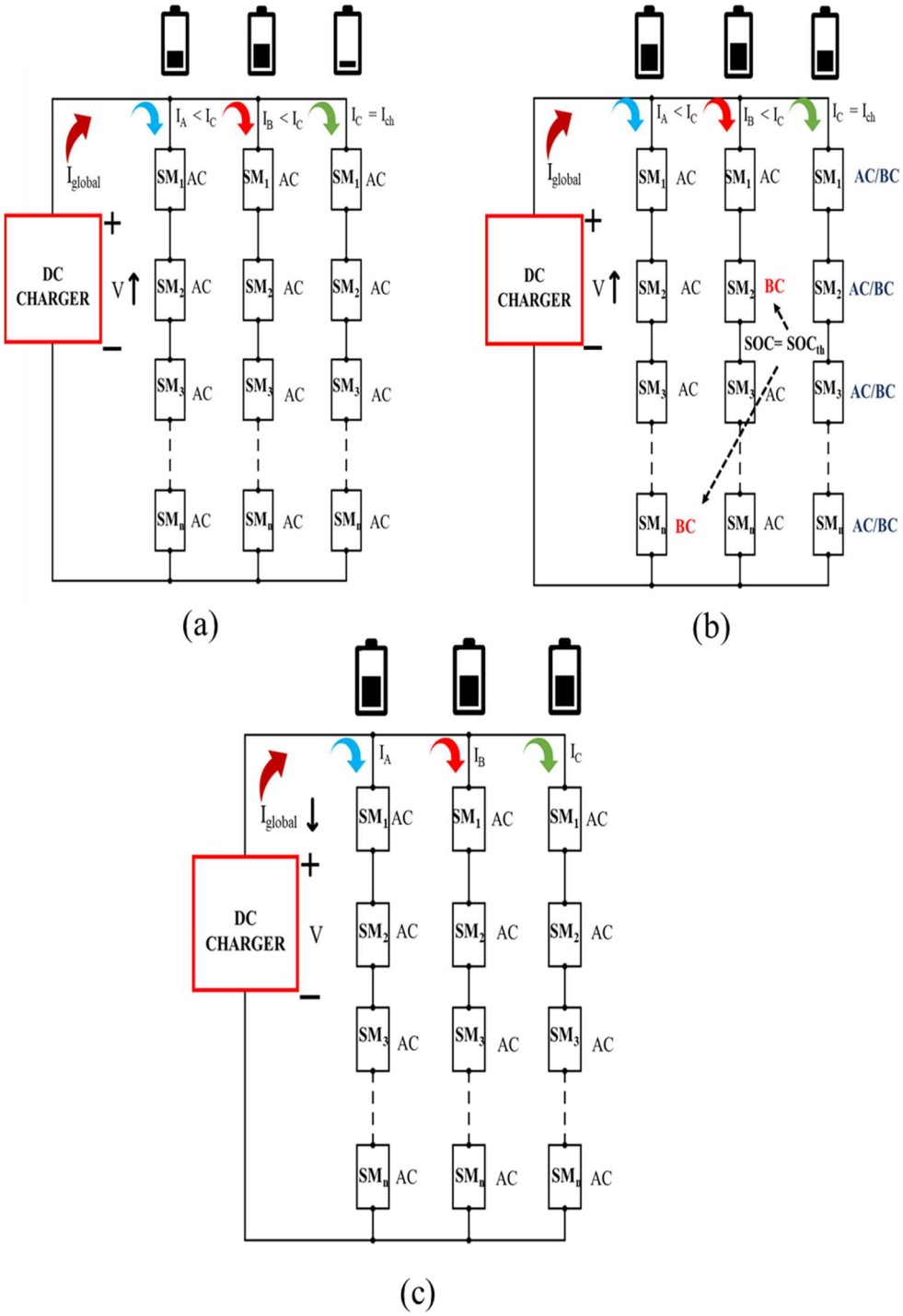

Fig. 3 – (a) All submodules are in active configuration (AC). The output voltage of the charger is controlled in order to have the nominal current flowing in the phase C, the less charged one. (b) Two submodules are set in bypass configuration (BC) to exclude their battery modules. The submodules of the phase C are periodically alternated to have always in conduction n-1 submodules. (c) - The CV phase starts: all submodules are in active configuration; the charger provides a fixed voltage.

IV. Simulations

The simulations are carried out in Simulink, MATLAB. The number of submodules per phase is chosen to be 3, as it is considered an optimized configuration for CHB in automotive application [16]. The

simulated battery modules are made by serial and parallel connections of the MOLICEL battery cell. Its characteristics and the details about the battery modules simulated are shown in Table I.
The charging process of the MOLICEL has been modelled with the discharging curves given by the datasheet. The difference between the mechanical parameters of the battery cells is taken into account by varying the actual resistance and capacity with a normal distribution respect to a standard deviation.

Simulation results

Fig.5a and Fig.5b show the battery modules SOCs and the charging currents through the phases, respectively. The initial SOCs are less than SOC_{th}, therefore, the CC phase starts for all the battery modules. As soon as one battery module reaches SOC_{th}, the CC phase is eligible for only two battery modules per phase. The algorithm alternates periodically the remaining battery module per phase, so that the charging process is balanced. When the battery modules of the three phases reach SOC_{th}, the CV phase is eligible and starts for all the phases.
Despite of the significant difference between the initial SOC values – around 55%- at the end of the charging process, the maximum difference of SOC values between all the battery modules is less than 1.5%. Indeed, after the initial SOC values gaps are fulfilled, the balanced dynamic is achieved by alternating the activation of the submodules, which guarantees that the battery modules in one phase can be charged in a balanced way.
Meanwhile, the phase currents follow the maximum current control: the less charged phase is crossed by the highest charging current. When two or more submodules are alternated, the phase currents show a small ripple due to the different equivalent impedance seen by the charger, as it is shown in Figure 5b.

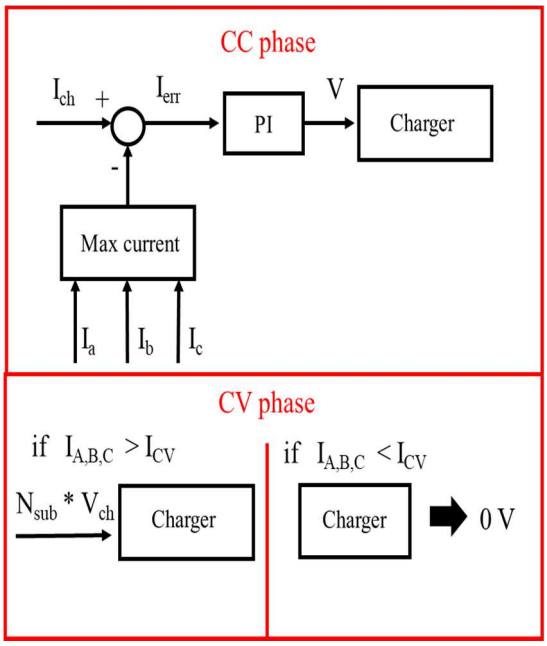

Fig. 4 – Implemented control according to the charging protocol phase.

TABLE I. SIMULATION PARAMETER

Battery cell characteristics	
Battery cell capacity	2.6 Ah
Battery cell voltage	3.6 V
Battery cell maximum voltage	4.2 V
Nominal charging current	2.6 A
Maximum internal resistance	20 mΩ
Battery module composition	
N° of battery cells in series	16
N° of battery cells in parallel	40
Capacity	104 Ah
Nominal voltage	57.6 V
Nominal charging current I_{ch}	104 A
Maximum Voltage	67.2 V
Minimum Voltage	40 V

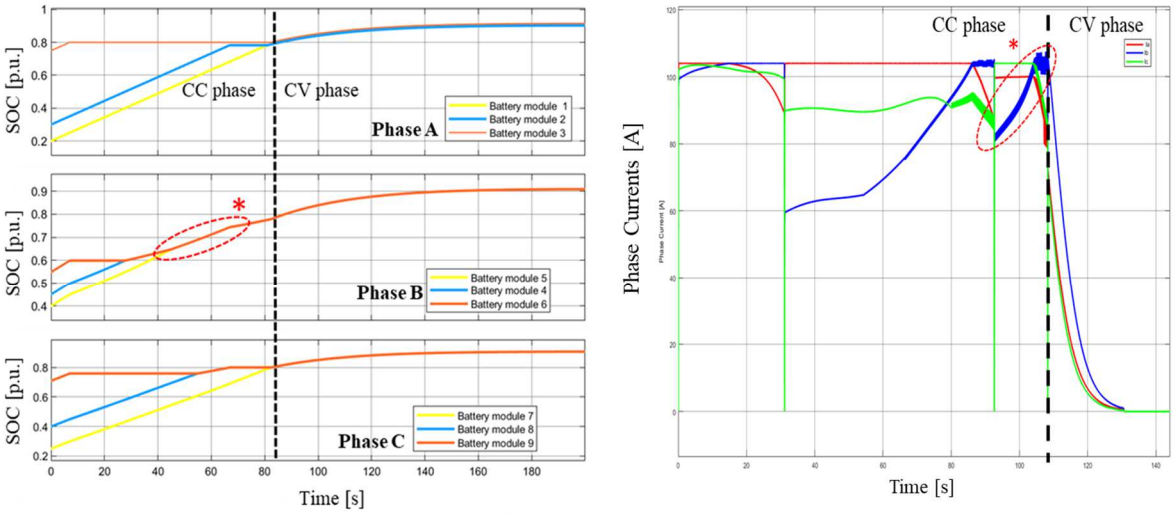

(a) (b)

Fig. 5 – (a)The SOC trend for the battery modules is shown. *SOC balanced dynamic. (b) Charging currents through the phases A, B and C. *The phase currents show a ripple due to the alternation of the submodules.

V. Experimental results

The experimental activities are carried out with a single-phase CHB, with two submodules. Instead of battery modules, a MOLICEL INR-18650-P26A battery cell is charged with the presented protocol. Fig.6 shows the experimental setup: the DC charger is implemented with a Buck-converter connected to the two H-bridge. The algorithm is implemented through the utilization of the UCUBE platform [17]. Fig. 7a shows the estimated and measured voltages and the SOC values of both the battery cells, respectively. Fig. 7b shows the charger voltage and current, respectively.
The charging process is divided in 3 stages:

1) The initial SOC values are less than SOC_{th}: therefore, both battery cells are charged in CC phase. The charger voltage increases in order to keep a constant charging current value.
2) One battery cell reaches $SOC_{th,}$ therefore it is bypassed. The CC phase continues for the other battery cell. As it is shown in Fig.8, the charger voltage drops to around 5 V.
3) When the second battery cell reaches SOC_{th} as well, the CV phase starts and terminates when the charging current drops below 0.1 A. The charger voltage is constant, while the current exponentially decreases.

The measurement of the battery cells has been added to demonstrate the validity of the charging algorithm. Indeed, the difference between the estimation and the calculation is completely negligible. Finally, the SOCs of the two battery cells converges at the same value, equal to 0.87%.

VI. Conclusion

This paper proposes a new perspective for EV battery charging architectures using multilevel converters. Instead of using the multilevel converter for the charging station, a CHB is employed as the power converter for the powertrain. Moreover, compared to the other research work, the three- phase CHB is connected to a unique DC charger in order to perform a simultaneous charging process for all battery modules within the converter. The novel algorithm here presented is able to control the charging process of all battery modules installed without the need of extra middle stage converters. The simulation and experimental work here presented show the feasibility and the validity of the algorithm.

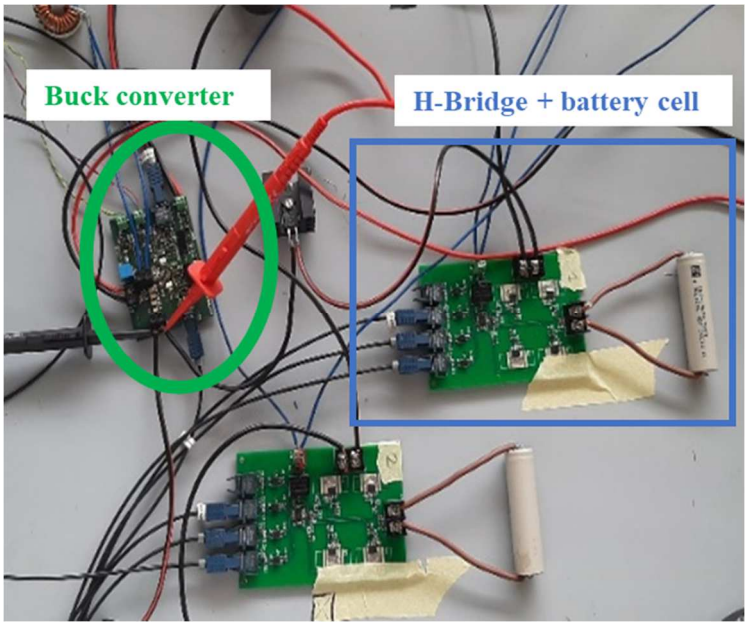

Fig. 6 - Experimental setup

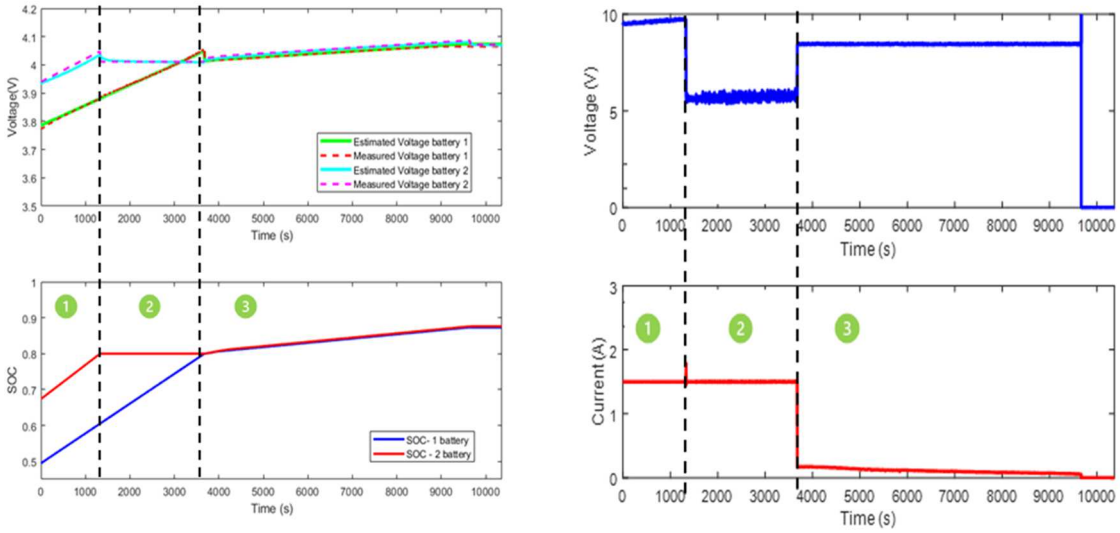

(a) (b)

Fig. 7 – Up: the measured and estimated voltage for the two battery cells. Bottom: estimated SOC values for both battery cells. (b) Charger (buck-converter) voltage (up) and current (bottom) output .

References

[1] J. O. Estima and A. J. Marques Cardoso, "Efficiency Analysis of Drive Train Topologies Applied to Electric/Hybrid Vehicles," in IEEE Transactions on Vehicular Technology, vol. 61, no. 3, pp. 1021-1031,March 2012, doi: 10.1109/TVT.2012.2186993.

[2] E. Knischourek, K. Muehlbauer and D. Gerling, "Power losses reduction in an electric traction drive at partial load operation," 2012 IEEE International Electric Vehicle Conference, 2012, pp. 1-5, doi: 10.1109/IEVC.2012.6183196.

[3] F. Chang, O. Ilina, M. Lienkamp and L. Voss, "Improving the Overall Efficiency of Automotive Inverters Using a Multilevel Converter Composed of Low Voltage Si mosfets," in IEEE Transactions on Power Electronics, vol 34, no. 4, pp. 3586-3602, April 2019, doi: 0.1109/TPEL.2018.2854756.

[4] A. Poorfakhraei, M. Narimani and A. Emadi, "A Review of Multilevel Inverter Topologies in Electric Vehicles: Current Status and Future Trends," in IEEE Open Journal of Power Electronics, vol. 2, pp. 155-170, 2021, doi: 10.1109/OJPEL.2021.3063550.

[5] M. Quraan, T. Yeo and P. Tricoli, "Design and Control of Modular Multilevel Converters for Battery Electric Vehicles," in IEEE Transactions on Power Electronics, vol. 31, no. 1, pp. 507-517, Jan. 2016, doi: 10.1109/TPEL.2015.2408435.

[6] G. Tresca, R. Leuzzi, A. Formentini, L. Rovere, N. Anglani and P. Zanchetta, "Reconfigurable Cascaded Multilevel Converter: A New Topology For EV Powertrain," 2021 IEEE Energy Conversion Congress and Exposition (ECCE), 2021, pp. 1454-1460, doi: 10.1109/ECCE47101.2021.9595741.

[7] R. Hariri, F. Sebaaly, C. Ibrahim, S. Williamson and H. Y. Kanaan, "A Survey on Charging Station Architectures for Electric Transportation," IECON 2021 – 47th Annual Conference of the IEEE Industrial Electronics Society, 2021, pp. 1-8, doi: 10.1109/IECON48115.2021.9589396.

[8] M. Safayatullah, M. T. Elrais, S. Ghosh, R. Rezaii and I. Batarseh, "A Comprehensive Review of Power Converter Topologies and Control Methods for Electric Vehicle Fast Charging Applications," in IEEE Access, vol. 10, pp. 40753-40793, 2022, doi: 10.1109/ACCESS.2022.3166935.

[9] A. Gholizad and M. Farsadi, "A Novel State-of-Charge Balancing Method Using Improved Staircase Modulation of Multilevel Inverters," in IEEE Transactions on Industrial Electronics, vol. 63, no. 10, pp. 6107-6114, Oct. 2016, doi: 10.1109/TIE.2016.2580518.

[10] C. Young, N. Chu, L. Chen, Y. Hsiao and C. Li, "A Single-Phase Multilevel Inverter With Battery Balancing," in IEEE Transactions on Industrial Electronics, vol. 60, no. 5, pp. 1972-1978, May 2013, doi: 10.1109/TIE.2012.2207656.

[11] A. Moeini and S. Wang, "The state of charge balancing techniques for electrical vehicle charging stations with cascaded H-bridge multilevel converters," 2018 IEEE Applied Power Electronics Conference and Exposition (APEC), 2018, pp. 637-644, doi: 10.1109/APEC.2018.8341079.

[12] Z. Zheng, K. Wang, L. Xu and Y. Li, "A Hybrid Cascaded Multilevel Converter for Battery Energy Management Applied in Electric Vehicles," in IEEE Transactions on Power Electronics, vol. 29, no. 7, pp. 3537-3546, July 2014, doi: 10.1109/TPEL.2013.2279185.

[13] S. Wang, R. Teodorescu, L. Mathe, E. Schaltz and P. Dan Burlacu, "State of Charge balancing control of a multi-functional battery energy storage system based on a 11-level cascaded multilevel PWM converter," 2015 Intl Aegean Conference on Electrical Machines & Power Electronics (ACEMP), 2015 Intl Conference on Optimization of Electrical & Electronic Equipment (OPTIM) & 2015 Intl Symposium on Advanced Electromechanical Motion Systems (ELECTROMOTION), 2015, pp. 336-342, doi: 10.1109/OPTIM.2015.7427002.

[14] P. Keil, A. Jossen, “Charging protocols for lithium-ion batteries and their impact on cycle life—An experimental study with different 18650 high-power cells”, Journal of Energy Storage, vol. 6, pp. 125-141, 2016, ISSN 2352-152X.

[15] Wen-Yeau Chang, "The State of Charge Estimating Methods for Battery: A Review", International Scholarly Research Notices, vol. 2013, Article ID 953792, 7 pages, 2013. https://doi.org/10.1155/2013/953792

[16] F. Roemer, M. Ahmad, F. Chang and M. Lienkamp, “Optimization of a Cascaded H-Bridge Inverter for electric vehicle applications including cost consideration”, *Energies,* 2019, 12, 4272.

[17] A. Galassini, G. Lo Calzo, A. Formentini, C. Gerada, P. Zanchetta and A. Costabeber, "uCube: Control platform for power electronics," 2017 IEEE Workshop on Electrical Machines Design, Control and Diagnosis (WEMDCD), 2017, pp. 216-221, doi: 10.1109/WEMDCD.2017.7947749.